CHEMICAL REACTION OF METAL-CARBON BINARY CLUSTER ANIONS BY FT-ICR MASS SPECTROMETER

Shigeo Maruyama, Masamichi Kohno and Shuhei Inoue

Engineering Research Institute and Department of Mechanical Engineering,
The University of Tokyo
2-11-16 Yayoi, Bunkyo-ku, Tokyo 113-8656, Japan

Metal-carbon binary clusters generated by the laser vaporization of metal-doped carbon materials used for macroscopic production of endohedral metallofullerene or SWNTs were studied. Positive and negative clusters generated by the laser-vaporization supersonic-expansion cluster beam source were directly injected to the FT-ICR mass spectrometer. Depending on the metal species, the generated cluster distributions were drastically different. The chemical reaction of these clusters with NO was used as the probe of the structure of clusters. LaC_{2n}^-, ScC_{2n}^- and YC_{2n}^- from La-doped, Sc-doped and Ni/Y-doped carbon samples, respectively, were much less reactive to NO compared with pure carbon clusters. On the other hand, NiC_n^- from Ni/Co-doped and Ni/Y-doped materials was much more reactive than pure carbon clusters. Through comparisons with the molecular dynamics simulations, it was speculated that La, Sc and Y were inside the annealed "random-cage" carbon structure even at small size as $M@C_{44}$. Through experiments of Ni/Co and Ni/Y doped samples for SWNT generation, carbon clusters with Y atom inside the random cage and only a small amount of carbon clusters with a Ni atom were observed. However, a drastic enhancement of even-odd alternations in pure carbon distribution was observed. The efficient generation of "random cage" structures starting from C_{36} might be the important step in the generation mechanism of SWNT.

INTRODUCTION

After the discovery of C_{60} by Kroto *et al*. (1) in 1985, macroscopic amount of empty fullerene (2,3), endohedral metallofullerene (4-7), higher fullerenes (8) and carbon nanotubes (9) were successively produced and isolated. Recently, the high quality generation of single walled nanotubes (SWNTs) (10-12) has demonstrated new possibilities of applications. Despite the expectations of applications, it is still difficult to obtain macroscopic amount of metallofullerene due to the extremely low yield of generation. In order to find the optimum generation condition, the understanding of the formation mechanism is inevitable. According to experimental studies, the transition metals such as Ca, Sr, Va, Sc, Y and lanthanides can be encapsulated inside the fullerene cage. On the other hand, Ni, Co, or Fe are required to generate the SWNTs (10-12), although they are not assigned to be encapsulated in the fullerene cage. Here, effects of these metal atoms on the growth process of carbon clusters leading to endohedral metallofullerene or SWNT are still unknown.

We have performed molecular dynamics simulations of the clustering process of carbon atoms to investigate the empty fullerene formation mechanism (13,14). Here, the

formation of perfect C_{60} structure was demonstrated by giving sufficient annealing time after the cluster growth through random collisions. Based on these results, a formation model of empty fullerene through "random-cage" structure was proposed (14). The formation process of metallofullerene was also studied using the similar molecular dynamics simulations in our previous reports (15-17). The difference of the growth processes among La, Sc and Ni containing systems were studied to investigate the effect of metal atoms.

In order to verify the idea from the molecular dynamics simulations, we had studied the metal-carbon binary clusters obtained by the laser-vaporization supersonic-expansion cluster beam source (15). Fourier Transform Ion Cyclotron Resonance (FT-ICR) mass spectrometer directly connected to the cluster source was implemented (15) with the same basic design concept to the apparatus at Rice University (18). We have shown that positive La-C, Y-C, Sc-C, Gd-C, and Ce-C binary clusters commonly showed strong MC_{2n}^+ signal in the range of $36 < 2n < 76$ with intense magic numbers at MC_{44}^+, MC_{50}^+ and MC_{60}^+ (15).

In this paper, in order to probe the structure of clusters appearing in mass spectra, the reactivity of negative carbon clusters and metal-carbon binary clusters to nitric oxide was measured. In addition to metal atoms for endohedral metallofullerene, Ni/Co-doped and Ni/Y-doped carbon samples for SWNT generation were vaporized. Comparing these cluster experiments with molecular dynamics simulations, generation mechanism of endohedral metallofullerene and SWNTs are discussed. It is suggested that the important role of metal atoms determining the final products as endohedral metallofullerene or SWNTs is apparently in the stage of small metal-carbon binary clusters.

EXPERIMENTAL APPARATUS AND PROCEDURE

The FT-ICR mass spectrometer and chemical reaction system implemented in this study is based on the design in Smalley's group at Rice University (18-20) and the detailed characteristics are described in elsewhere (15). Fig. 1 and Fig. 2 show the cluster beam source and direct injection FT-ICR apparatus, respectively. The cluster beam was generated outside of magnetic field by the laser-vaporization cluster beam source shown in Fig. 1. A pulsed gas valve, the sample motion mechanism and a skimmer were installed in a 6-inch 6-way UHV cross. A metal-doped carbon sample disk was vaporized by the focused beam of Nd: YAG laser (2nd Harmonics) while timed pulsed gas was injected to the nozzle. In the atmosphere of helium gas, vaporized atoms condensed to clusters, and then, were carried and cooled by the supersonic expansion of helium gas. The cluster beam was directly injected to the

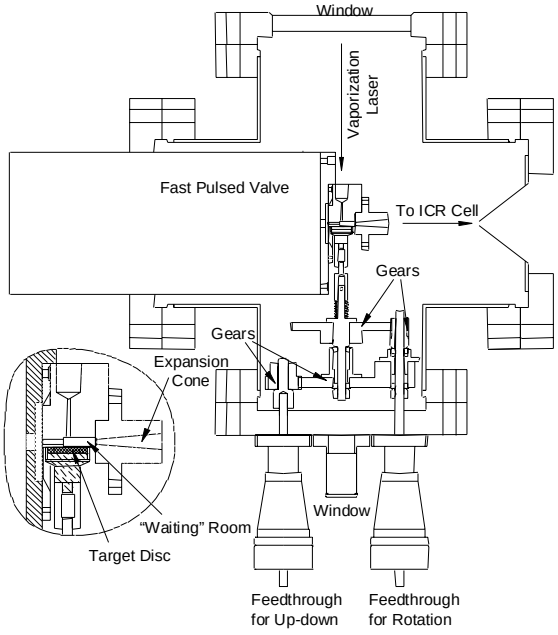

Fig. 1 Laser-vaporization cluster beam source

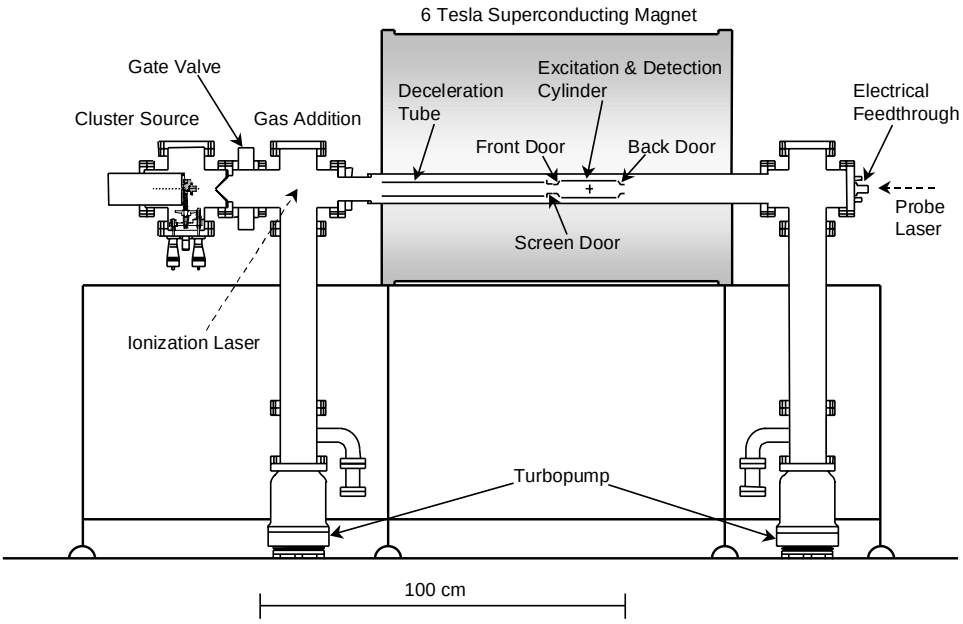

Fig. 2 FT-ICR mass spectrometer directly connected with laser-vaporization cluster beam source.

magnetic field through a skimmer with the opening diameter of 2 mm and a deceleration tube (18).

The FT-ICR is the unique mass spectroscopy based on the ion-cyclotron motion of clusters in a strong magnetic field. In principle, extremely high mass-resolution at high mass-range such as resolution of 1 amu at 10,000 amu range can be obtained. Furthermore, since the ions can be trapped in the vacuum for a few minutes, it is possible to perform the chemical reaction experiments. The ICR cell, 42 mm I.D. 150 mm long cylinder was placed in a stainless tube (SUS316) of 84 mm I.D. which penetrated the homogeneous 5.87 Tesla superconducting magnet commercially available for NMR. Two turbo-pumps (300 ℓ / s) fore-pumped by a smaller turbo-pump of 50 ℓ / s were placed at the floor in order to avoid the effect of strong magnetic field. The typical background pressure was 3×10^{-10} Torr.

The typical chemical reaction procedure was as follows:

- Cluster beam was injected in 10 Hz for 10 s to the ICR cell. Size range of cluster ions was roughly selected by the deceleration voltage (18).
- The kinetic energy of clusters was thermalized with room temperature argon gas. This procedure was skipped for present study.
- Unwanted clusters were over-excited and excluded from ICR cell by SWIFT (Stored Waveform Inverse Fourier Transform) excitation (21).
- Remaining clusters were thermalized with room temperature argon gas at 10^{-5} Torr for 10 s.
- Nitric oxide gas was injected to the cell by 10 Hz pulsed valve for a fixed period. The pulse value was adjusted so that the pressure at the ICR cell chamber became at 10^{-5} Torr for unreactive clusters and 10^{-7} Torr for reactive clusters.
- After pumping out for about 8 to 10 s, cluster ions were excited to detect the mass distribution.

RESULTS AND DISCUSSIONS

In order to study the interaction of metal atoms with carbon clusters during the formation process of endohedral metallofullerene or SWNTs, 4 different sample materials were used in the cluster beam source. Two of them were composite disks of La/C and Sc/C optimized for the macroscopic generation of endohedral metallofullerene and 2 others were Ni/Co/C and Ni/Y/C composites usually used for the generation of SWNTs in laser-oven technique and arc-discharge technique, respectively. All of these samples were commercially supplied from Toyo Carbon Co. (Tokyo). Graphite powder mixed with metal oxides and some binder were pressed and thermally treated. The nominal atomic mixing rates were 0.8 % La for La/C, 0.8 % Sc for Sc/C, 0.6 % Ni and 0.6 % Co for Ni/Co/C, and 4.2 % Ni and 1.0 % Y for Ni/Y/C.

Contamination with Hydrogen Atoms for La-Doped Carbon Sample

Fig. 3 compares positive and negative ion mass spectra generated from the La/C sample. As we had already reported (15), cluster ions with one La atom and even number of carbon atoms starting from LaC_{36}^{+} were observed for positive mass spectrum. And, LaC_{44}^{+}, LaC_{50}^{+}, and LaC_{60}^{+} were observed to be especially intense signal. Pure carbon clusters were barely observed in the positive spectrum except for the very small C_{60} signal (considerable expansion of Fig. 3(a) is necessary to see C_{60} peak). Since the ionization potential of metal-carbon binary clusters are expected to be considerably lower than pure carbon clusters, the amount of pure carbon clusters may not be negligible for neutral clusters. Since negative clusters are believed to reflect the abundance of neutral clusters, we will concentrate on negative clusters in this paper. In negative cluster distribution in Fig. 3(b), small pure carbon clusters up to about C_{60} are observed in addition to LaC_{2n}^{-} clusters. The distribution of pure carbon clusters seems to be the same as the typical negative mass spectrum obtained from pure-graphite sample. Small even-

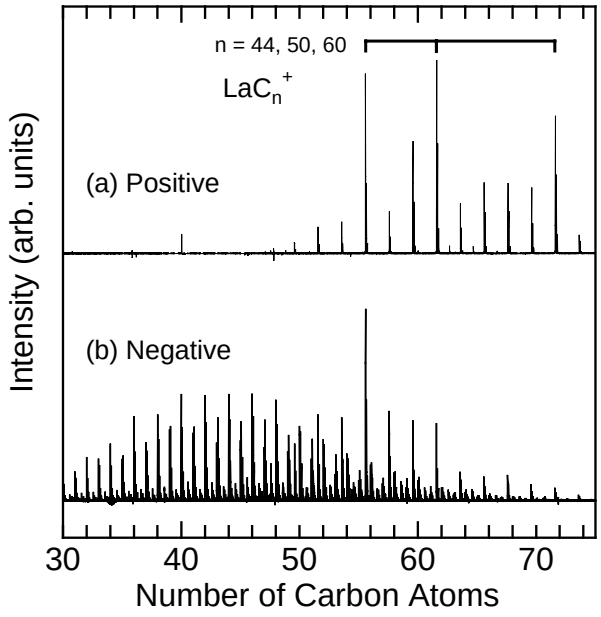

Fig. 3 Positive and negative clusters from La/C mixture as injected to ICR cell.

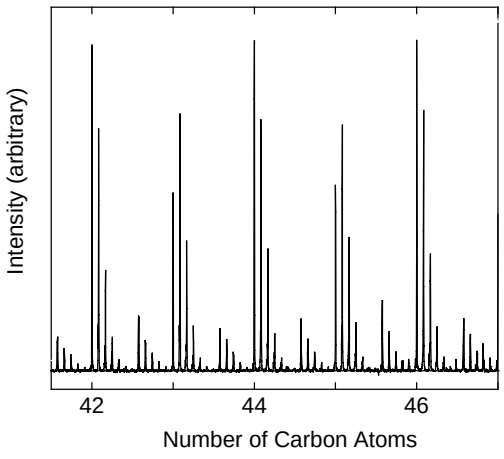

Fig. 4 Even-odd difference of hydrogen contamination of pure carbon clusters.

Table 1 Estimated amount of hydrogen contamination

	C_n	C_nH	C_nH_2	C_nH_3
n: even	71.6%	19.6%	7.2%	1.6%
n: odd	47.0%	43.0%	6.4%	3.6%

odd alternations in pure carbon clusters observed in Fig. 3(b) were an artifact due to the hydrogen contamination as follows.

Fig. 4 shows the expanded view of Fig. 3(b). Striking difference in the fine mass distribution from the expectation due to the natural abundance of carbon isotopes is apparent for odd-numbered clusters. By decomposing the fine mass structure, number of hydrogen atoms attached to each clusters were measured. The percentages of pure carbon cluster and with 1-3 hydrogen-contaminated clusters were summarized in Table 1. Here, average values for even and odd numbered clusters in the range C_{42} through C_{51} are shown. More than half of odd numbered clusters were contaminated with more than one hydrogen atoms, in contrast to that 70 % of even numbered clusters were pure carbon clusters. It should be noticed that C_nH_2 percentage for even numbered clusters were larger than for odd-numbered clusters. It should be also noticed that the largest signal intensity for odd-numbered clusters are less because of this hydrogen contamination, but the integrated intensity of each cluster size were almost the same for even and odd clusters. So, the even-odd alternations of intensity observed in Fig. 3(b) were an artifact. The reason of hydrogen contamination was not clear. Even though the careful cleaning of helium gas line is often omitted for carbon cluster experiments, the contamination by hydrogen is usually not likely for carbon clusters. It may be that the effect of water in the helium gas line or the surface of the target material was enhanced by the catalytic effect of La atoms.

Reaction of Pure Carbon Clusters to NO

Since the even-odd alternations of the hydrogen contamination reaction were so clear, the pure carbon clusters were first examined by the following reaction experiments with NO prior to metal-carbon binary clusters. Fig. 5 shows the mass spectra in each stage of reaction experiments. Fig. 5(a) shows the cluster distribution as injected from the cluster beam source. Fig. 5(b) shows the result of mass selection of C_{37} and C_{40} as typical odd and even numbered clusters by SWIFT technique, followed by the thermalization to the room temperature by collisions of argon gas at 10^{-5} Torr for 10 s. Then, NO gas at 10^{-5} Torr was exposed for 1, 3, 10 s, as shown in Fig. 5 (c), (d), (e), respectively. Apparently,

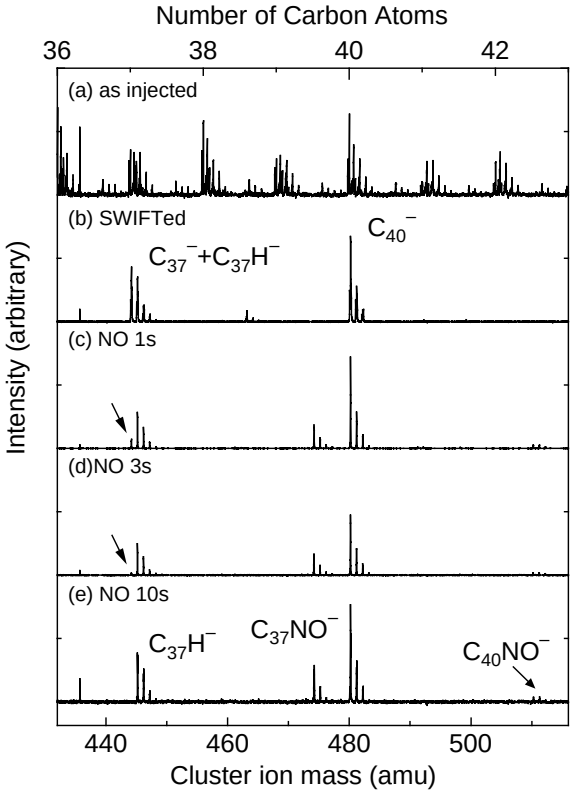

Fig. 5 Reaction of carbon clusters with NO.

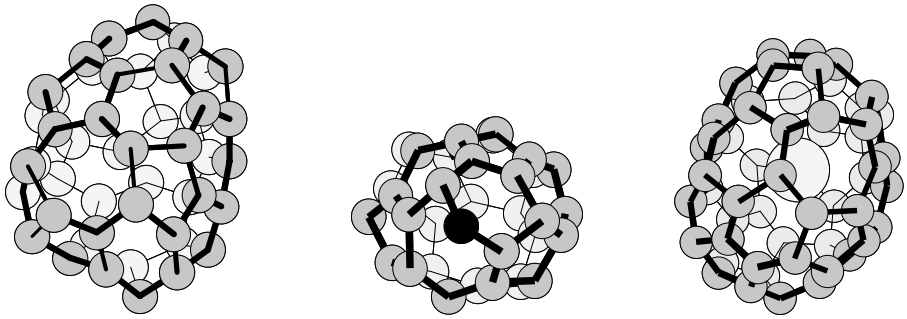

(a) C_{48} (b) C_{33} (c) La@C_{54}

Fig. 6 Typical random-caged structures picked up from the molecular dynamics simulations. (a) C_{48} without dangling bonds. (b) C_{33} with one dangling bond (in black atom). (c) Even-numbered carbon cluster with La atom inside: La@C_{54}.

the C_{37}^- was much more reactive to NO compared with C_{40}^- and gave considerable amount of product ion $C_{37}NO^-$. A careful study of the fine isotropic structure reveals the much striking feature of the reactivity. The lowest mass signal of C_{37}^- due to $^{12}C_{37}$ (444 amu, marked by arrows) was reduced to about one fourth after 1 s reaction and was almost completely gone after 3 s reaction. This means that non-contaminated C_{37}^- was almost completely reacted away at 3 s reaction and $C_{37}H^-$ and C_{40} remained almost unreacted. Systematic studies of other pure carbon clusters showed the similar results; odd numbered and even numbered clusters behaved as C_{37} and C_{40}, respectively.

Random Cage Structure Predicted from Molecular Dynamics Simulations

A clear explanation of the even-odd difference in the hydrogen contamination and the reactivity to NO, especially with and without a hydrogen atom was obtained from the comparison with the molecular dynamics simulations (14). By the classical molecular dynamics simulation at high temperature at 2500 K, carbon clusters with 30 to 60 atoms annealed to almost spherical random-cage structure as shown in Fig. 6 (a) and (b). Starting from a random structure, most of clusters tried to reduce the number of dangling bonds. At this stage, even numbered clusters always had 0, 2, 4, … atoms with a dangling bond (an atom with 2-bonds), and odd numbered clusters had 1, 3, 5, … atoms with a dangling bond. Finally, at least one dangling bond remained for odd numbered clusters. Our previous simulation of the annealing of C_{60} and C_{70} successfully to IPR fullerene structure (14) was also consisted of 3 stages, dangling bonds were removed first, all faces became pentagons and hexagons, and finally transformed to IPR structure through Stone-Wales transformations. The number of dangling bonds for even and odd numbered clusters can be very clearly explained by the Euler's theorem of geometry. For a closed polyhedral structure, there is a following relation between number of faces *f*, number of edges *e*, number of vertices *v*.

$$f + v = e + 2 \tag{1}$$

There are additional relations between number of pentagons f_5 and number of hexagons f_6 for a fullerene.

$$2e = 5f_5 + 6f_6, \;\; 3v = 5f_5 + 6f_6 \tag{2}$$

As a result, it is well known that the number of pentagon is always 12 and number of total atoms is even as

$$f_5 = 12,\ v = 20 + 2 f_6 \tag{3}$$

However, if we consider that all atoms had three bonds (no dangling bonds), it can be directly derived that number of atoms must be even regardless of size of faces. The condition that all atoms had three bonds can be expressed as

$$e = \frac{3}{2} v\,. \tag{4}$$

Only with this condition (without the assumption in eq. (2)) Euler's theorem can be rewritten to

$$v = 2 f - 4\,, \tag{5}$$

which means that number of atoms (vertices) must be even. This condition explains the molecular dynamics annealing that all dangling bonds were removed for even numbered clusters before the faces became only pentagons and hexagons. Considering the number of atoms with a dangling bond (atoms with only 2 bonds) as v_2, with number of atoms with 3 bonds v_3, the relation in eq. (4) is modified to

$$e = \frac{3}{2} v_3 + v_2\,. \tag{6}$$

Then, the equation (5) is modified to

$$v = 2 f - 4 + v_2\,. \tag{7}$$

This means that when total number of atoms in a cluster $v = v_2 + v_3$ is even, number of atoms with a dangling bond v_2 is even, and when v is odd, v_2 is odd. Naturally, the molecular dynamics results obeyed this relation with a tendency to reduce the number v_2. Since odd numbered clusters had at least one dangling bond, contamination with a hydrogen atom can be enhanced. Furthermore, slightly larger C_nH_2 for even numbered cluster in Table 1 can be explained as the structure with $v_2 = 2$. The reactivity of NO to pure carbon clusters can be interpreted that NO reacted to the atom with a dangling bond. And, a hydrogen atom attached to odd-numbered cluster can block the attack of NO.

<u>Lanthanum-Carbon Binary Clusters</u>

Fig. 7 compares the reactivity of La-C binary cluster LaC_{44}^- to typical odd and even numbered pure carbon clusters C_{44}^- and C_{47}^-. After 1 s reaction

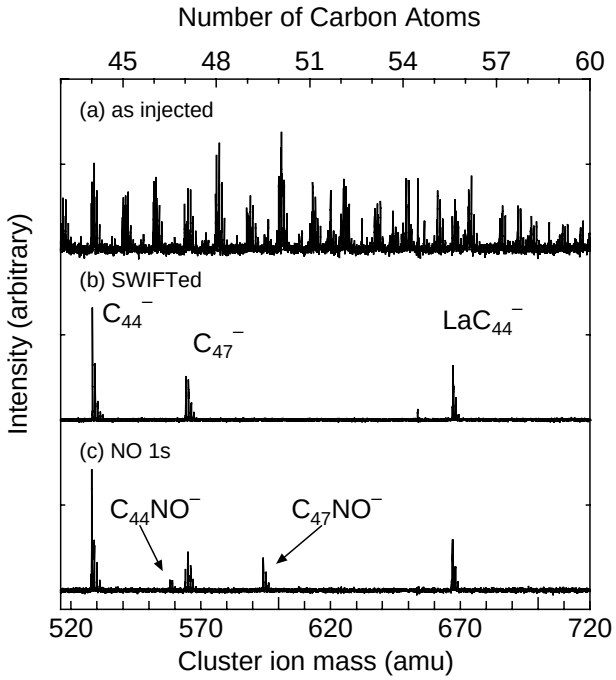

Fig. 7 Chemical reaction of LaC_{44}^- with NO compared with bare clusters. (a) As injected, (b) C_{44}^-, C_{47}^-, LaC_{44}^- clusters were selected, (c) After reaction with NO at 10^{-5} Torr.

with NO, reaction of C_{47} and a little bit of C_{44} were observed as in Fig. 7(c). However, the reaction of LaC_{44} was not observed. In general, it is expected to be more reactive if a metal atom is exposed to NO. The much less reactive LaC_{44}^- strongly suggests that La atom is inside the carbon cage. Furthermore, since La-C binary clusters with odd number of carbon atoms were much less abundant than even-numbered carbon atoms, it can be speculated that LaC_{2n} such as LaC_{44} are much better annealed than pure carbon clusters. If the La atom is inside the cage, the geometric consideration is completely the same as previous section. Fig. 6(c) shows a typical structure found in our molecular dynamics simulation. It is important to notice that the meta-stable structure with all carbon atoms with 3-coordinates bonding can be made for even-numbered carbon clusters even with a 7-membered ring as in Fig. 6(c).

Ni/Co Doped Carbon Material

The similar experiments were performed for the Ni/Co (0.6 at % Ni and 0.6 % Co) doped carbon material used for the laser-oven SWNT generation. Positive and negative mass spectra as injected from the cluster beam source are shown in Fig. 8. There was not a trace of Ni or Co in the positive mass spectrum and tiny signals of NiC_n and probably CoC_n were measured for negative spectrum as in Fig. 9 (expanded view of Fig. 8(b)). More drastic effect of doping of Ni/Co was observed in pure carbon cluster distribution, which will be discussed later. In Fig. 9, the signal of ^{58}Ni with 57.94 amu can be clearly distinguished with no overlap, but ^{59}Co with 58.93 overlaps with Ni-C binary cluster signal. The half of the signal next to NiC_n is most likely from CoC_n, though the precise decomposition is not easy for this low signal intensity. There was some even-odd difference in the signal intensity of NiC_n and CoC_n; these peaks were stronger for even-numbered carbon clusters. However, this even-odd difference seems to simply reflect the relative abundance of pure carbon clusters.

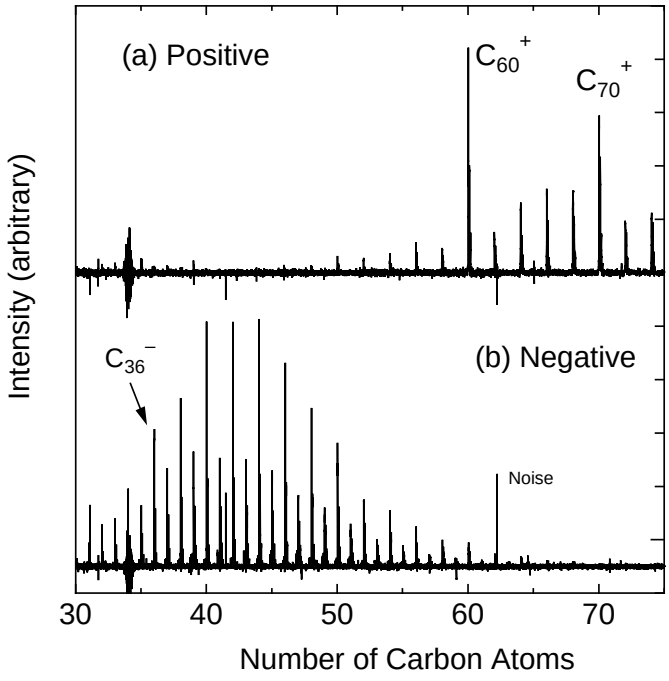

Fig. 8 As injected positive and negative clusters from Ni/Co/C Mixture

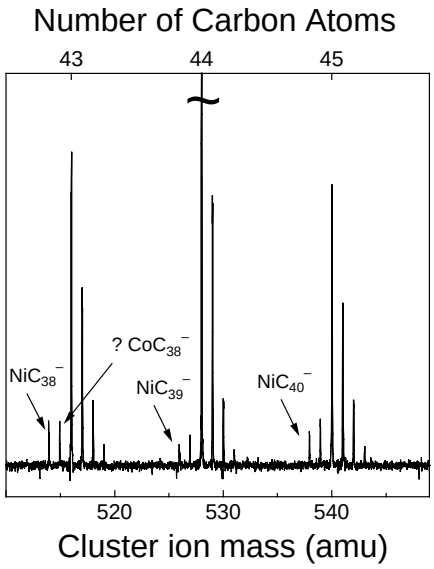

Fig. 9 Expanded view of Fig. 8(b).

The reaction experiments with NO were done without the selection of clusters because the signal level was so low. The reaction results with 10^{-7} Torr NO for 2 s and 10 s are shown in Fig. 10. The chemisorption of NO to NiC_n and CoC_n were observed much faster rate than pure carbon clusters. It should be noticed that the pressure of NO was 1/100 times compared with the case of LaC_n experiments. It seems that CoC_n reacted a bit faster than NiC_n. After the reaction for 10 s, the product of C_nNO gradually appeared.

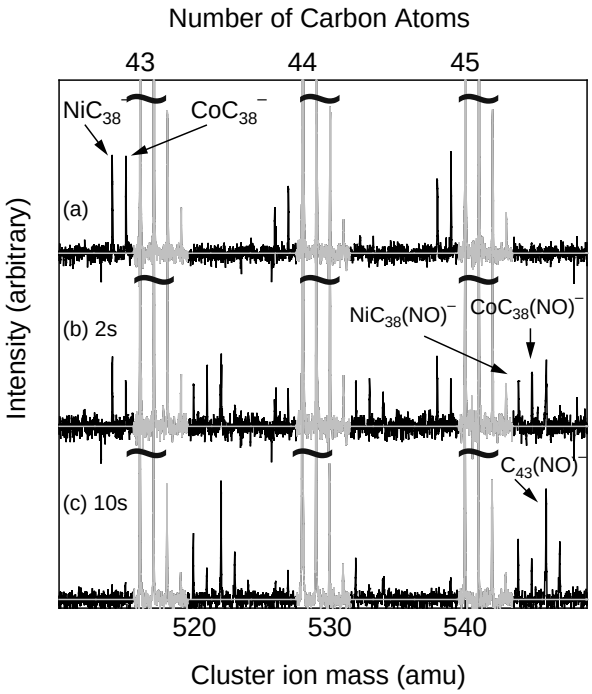

Fig. 10 Reaction of NiC_{38}^- and CoC_{38}^- with NO.

Ni/Y Doped Material

The Ni/Y (4.2 % Ni and 1.0 % Y) doped carbon material optimized for the arc-discharge SWNT generation was also studied. The positive mass spectrum shown in Fig. 11(a) was not distinguishable from the Y doped carbon material (0.8 % Y) used for the endohedral metallofullerene generation (15). Most of clusters had one Y atom and even numbered carbon atoms, and only small signals of pure carbon clusters such as C_{60}^+ and C_{70}^+ were observed. In the negative spectrum, however, small pure carbon clusters and Ni attached clusters in addition to YC_{2n} were observed. As shown in Fig. 12(a), abundance of Ni attached clusters were sometimes almost the half of odd-numbered pure clusters for around NiC_{40}, but Ni-attachment was not observed for large clusters more than 50 carbon atoms.

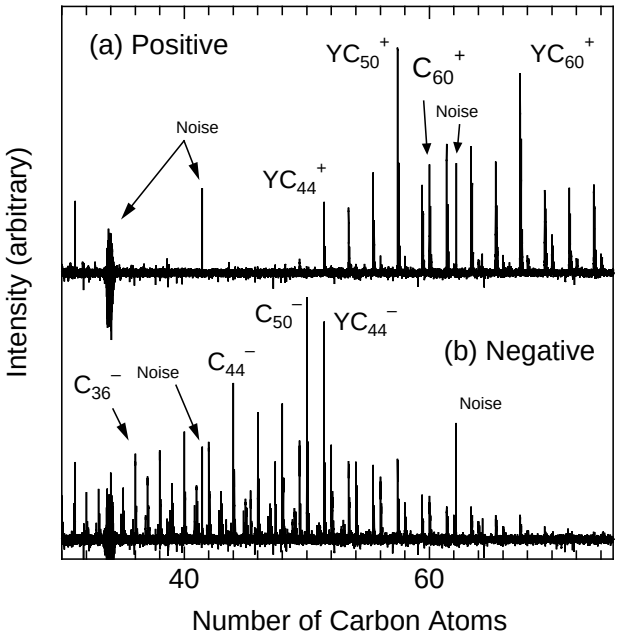

Fig. 11 As injected positive and negative clusters from Ni/Y-doped carbon material.

The reaction experiments with NO shown in Fig. 12 confirmed the very reactive feature of NiC_n^- cluster and much less reactive feature of YC_n^-. It is speculated that Y atom is inside the carbon cage and Ni is outside. Here, the molecular dynamics simulations (16,17) predicted a Ni atom attached on a face of 8-membered or larger ring as shown in Fig. 14. This may be a possible position of Ni or Co atom.

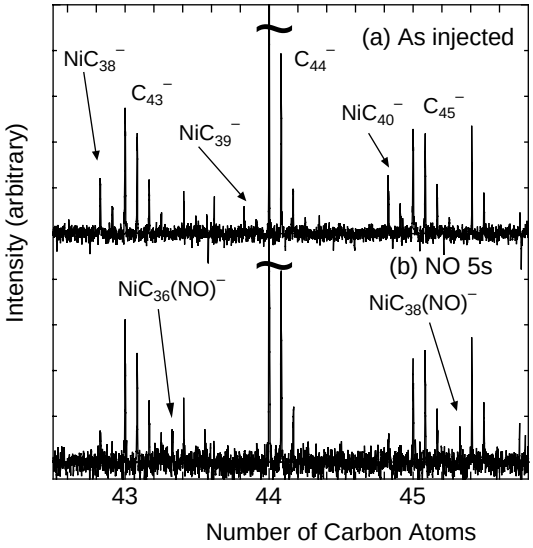

Fig. 12 Reaction of NiC_{38}^- with NO.

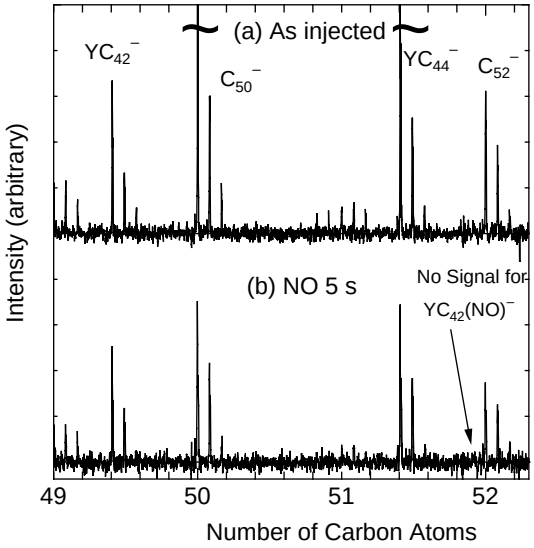

Fig. 13 Reaction of YC_{42}^- with NO.

Effect of Ni/Co and Ni/Y Mixtures on Pure Carbon Clusters

The effect of binary metal mixtures on generated pure carbon cluster distribution was very strong both for Ni/Co and Ni/Y doped carbon materials. The even-odd alternations in pure carbon cluster distribution in negative carbon clusters generated from Ni/Co doped sample shown in Fig 8 are unusual. Furthermore, magic numbers of C_{44}^- and C_{50}^- are clearly observed for Ni/Y doped sample in Fig. 11. These features are recognized as the tendency toward closing the random-cage structures, though it is not clear how metal atoms change these pure-carbon cluster distributions. One possible explanation may be that Ni or Co atoms interact with small carbon clusters to help the cage closure but are thrown away when the carbon size grows as large as 40 to 50 atoms where it can form stable random cage structure itself. The even-odd feature starts from C_{36}^- and it may be related to the special generation condition of C_{36} (22).

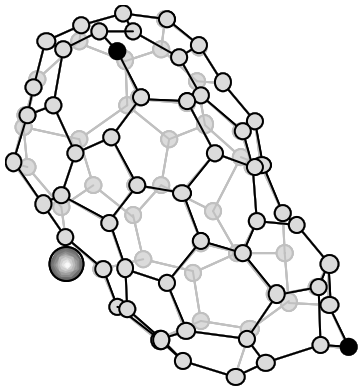

Fig. 14 Structure of NiC_{78} at 2500K by molecular dynamics simulation.

CONCLUSIONS

Metal-carbon binary clusters generated by the laser vaporization of metal-doped carbon materials used for macroscopic production of endohedral metallofullerene or SWNTs were studied. Positive and negative clusters generated by the laser-vaporization supersonic expansion cluster beam source were directly injected to the FT-ICR mass spectrometer. The chemical reaction of these clusters with NO was used as the probe of the structure of clusters. For the pure carbon clusters, clear difference of reactivity was observed between odd-numbered and even-numbered clusters, and one hydrogen atom made odd-numbered clusters less reactive. These experimental results were perfectly

explained by a consideration of number of dangling bonds based on the random-cage geometric structure predicted by the molecular dynamics simulations.

LaC_{2n}^-, ScC_{2n}^- and YC_{2n}^- from La-doped, Sc-doped and Ni/Y doped carbon samples, respectively, were much less reactive to NO compared with pure carbon clusters. On the other hand, NiC_n^- from Ni/Co-doped and Ni/Y doped materials was much more reactive than pure carbon clusters. Through comparisons with molecular dynamics simulations, it was concluded that La, Sc and Y were inside the annealed "random-cage" even at the size as small as $M@C_{44}$. Through experiments of Ni/Co and Ni/Y mixtures with carbon, clusters with Y atom inside the random carbon cage and only a small amount of carbon clusters with a Ni atom were observed. A drastic enhancement of even-odd alternations in pure carbon distribution was observed for these SWNT related materials. The efficient generation of random caged structures starting from C_{36} might be the important step in the generation mechanism of SWNT.

ACKNOWLEDGEMENTS

Part of this work was supported by Grant-in-Aid for Scientific Research (B) (No. 12450082) and for Encouragement of Young Scientists (No. 11750155) from the Ministry of Education, Science, Sports and Culture, Japan.

REFERENCES

1. H. W. Kroto, et al., *Nature*, **318**, 162 (1985).
2. W. Krätschmer, et al., *Nature*, **347**, 354 (1990).
3. R. E. Haufler, et al., *Proc. Mat. Res. Soc. Symp.*, **206**, 627 (1991).
4. Y. Chai, et al., *J. Phys. Chem.*, **95**, 7564 (1991).
5. H. Shinohara, et. al., *J. Phys. Chem.*, **96**, 3571 (1992).
6. K. Kikuchi, et al., *Chem. Phys. Lett.*, **216**, 23 (1993).
7. M. Takata, et al., *Nature*, **377**, 46 (1995).
8. K. Kikuchi, et al., *Chem. Phys. Lett.*, **188**, 177 (1992).
9. S. Iijima, *Nature*, **354**, 56 (1991).
10. S. Iijima and T. Ichihara, *Nature*, **363**, 603 (1993).
11. A. Thess, et al., *Science*, **273**, 483 (1996).
12. C. Journet, et al., *Nature*, **388**, 756 (1997).
13. Y. Yamaguchi and S. Maruyama, *Chem. Phys. Lett.*, **286**, 336 (1998).
14. S. Maruyama and Y. Yamaguchi, *Chem. Phys. Lett.*, **286**, 343 (1998).
15. S. Maruyama, et al., Fullerene Sci. Technol., **7**-4, 621 (1999).
16. Y. Yamaguchi and S. Maruyama, *Euro. Phys. J. D*, **9**-1,4, 385 (1999).
17. Y. Yamaguchi and S. Maruyama, *Fullerenes*, vol. **7**, ECS, 640 (1999).
18. S. Maruyama, L. R. Anderson and R. E. Smalley, *Rev. Sci. Instrum.*, **61**-12, 3686 (1990).
19. L. R. Anderson, S. Maruyama and R. E. Smalley, *Chem. Phys. Lett.*, **176**-3,4 348 (1991).
20. S. Maruyama, L. R. Anderson and R. E. Smalley, *J. Chem. Phys.*, **93**-7, 5349 (1990).
21. A. G. Marshall and F. R. Verdun, Fourier Transforms in NMR, Optical, and Mass Spectrometry, Elsevier, Amsterdam (1990).
22. C. Piskoti, J. Yarger and A. Zettl, *Nature*, **393**-25, 771 (1998).